EXPERIMENTAL ROBUSTNESS OF FXLMS AND DISTURBANCE-OBSERVER ALGORITHMS FOR ACTIVE VIBRATION CONTROL IN AUTOMOTIVE APPLICATIONS

Konrad Kowalczyk * **Ferdinand Svaricek** *

* *University of the German Armed Forces Munich, Department of Aviation and Space Engineering, Neubiberg, Germany, E-mail: konrad.kowalczyk@unibw-muenchen.de*

Abstract: The paper deals with two fundamentally different approaches for active control of engine-induced vibrations in automotive vehicles. On the one hand the well-known adaptive feedforward approach with a reference sensor is presented. On the other hand the use of feedback structures is also discussed. Both approaches for active vibration control have been simulated and tested intensively in a passenger car equipped with an active absorber system using electromagnetic actuators. On the basis of the obtained results some properties such as stability and robustness have been investigated and reported here.

Keywords: active vibration control, disturbance observer, state feedback, adaptive filter, robust control

1. INTRODUCTION

One of the applications of active vibration control is the use in engine mounting concepts, particularly since conventional mounts are approaching their inherent limitations. The standard approach is to isolate the engine and the transmission vibrations from the chassis with rubber or hydro mounts. This mount design is always a compromise between the conflicting requirements of acceptable damping and good isolation.

Rubber isolators work well (in terms of isolation) when the rubber exhibits low stiffness and little internal damping. Little damping, however, leads to a large resonance peak which can manifest itself in excessive engine movements when this resonance is excited (front end shake). These movements must be avoided in the engine compartments of today's cars where space is severly restricted. A low stiffness, while also giving good isolation, leads to a large static engine displacement and to a low resonance frequency. Classical mount design therefore tries to achieve a compromise between the conflicting requirements of acceptable damping and good isolation.

It has been recently reported that a significant comfort improvement can be achieved through applying active vibration control systems, see for example (Bohn *et al.*, 2004), (Sano *et al.*, 2002), (Svaricek *et al.*, 2001).

The motivation is the vibration attenuation of systems with periodic disturbances of a time–varying fundamental frequency, where the frequency varies from approximately 840 rpm at idle to approximately 6000 rpm.

Most of the control approaches rely on feedforward control strategies (either pure feedforward or combined with feedback). The feedforward signal is either taken from an additional sensor (usually an accelerometer in active vibration control) or generated artificially from measurements of the

fundamental disturbance frequency. Also, most approaches rely on adaptive control strategies such as the filtered–x LMS algorithm. This seems necessary as the characteristics of the disturbance acting upon the system are time–varying. While this works well in many applications, some critical issues such as convergence speed, tuning of the step size in the adaptive algorithm and stability remain.

A non-adaptive algorithm might have the benefit of a higher acceptance. Another advantage of a non-adaptive algorithm is that the behaviour of the closed loop system can be analysed independent of the input signals. In an adaptive algorithm, the optimal controller depends on the external signals that act upon the system; thus, it is very difficult to analyse the performance off-line.

Both kinds of algorithms have been implemented in an active control system for cancellation of engine-induced vibrations in several test vehicles. The focus of this paper is an analysis of some robustness properties of the two different control approaches. The paper is organized as follows: in Section 2 a brief description of an active vibration control system is presented. In the next Section a definition of a performance index for further analysis is given. Sections 4 and 5 describe two fundamentally different control techniques for active vibration control. In addition, some properties of both algorithms are presented. Finally, analysis of robustness to phase delay in the control signal, uncertainty in the plant transfer function magnitude and damping ratio are made and the simulation results are presented.

2. SYSTEM DESCRIPTION

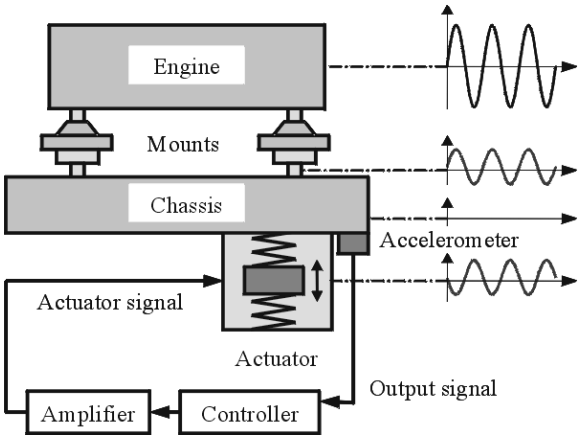

Fig. 1. Active absorber system configuration.

Figure 1 presents the concept of active vibration control in a vehicle using an active absorber. The disturbance force originating from the engine and transmitted to the chassis through the engine mounts is actively cancelled by an actuator force. The aim of the control system is to synthesise a waveform that is identical in magnitude, but 180 degrees out of phase from the original vibration signal, so that it cancels the effect of incoming excitation. (Lueg, 1936) (Kuo and Morgan, 1996).

Figure 2 shows the placement of actuator and sensor for an application with the objective to attenuate the transmission of engine–induced vibrations through the powertrain mounts into the chassis.

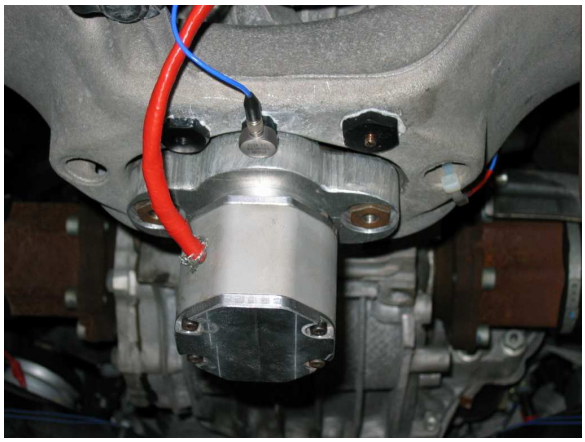

Fig. 2. Location of actuator and sensor in a test vehicle.

In active noise and vibration control, the reference signal is commonly zero; therefore, the controlled signal is also the error (with a sign reversal), which is why the output sensor is usually called the error sensor. The system structure consists of the power amplifier, electromagnetic actuator, acceleration sensor, and a dSPACE MicroAutoBox controller. The model of the plant (secondary path) is obtained through an identification experiment.

All the hardware components are combined together, so that they create a compact system. Figure 3 presents the components placed inside the car compartment.

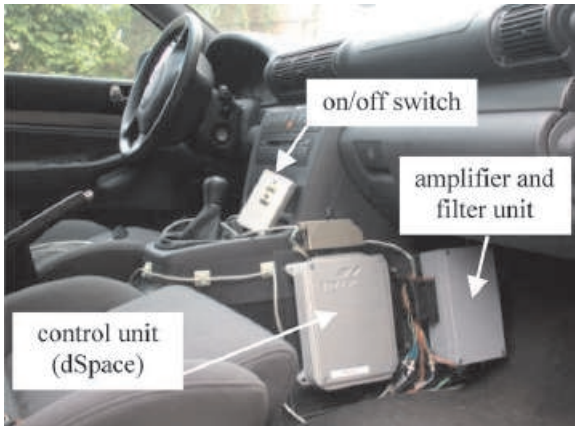

Fig. 3. Location of the electronic hardware in the test vehicle.

3. PERFORMANCE INDEX DEFINITION

The experimental performance index used in the analysis is defined as follows:

$$I = (1 - \frac{var(e_{ctr})}{var(e_{unctr})}) \cdot 100\%, \qquad (1)$$

where var is the statistical variance of the signal, e_{ctr} is the obtained error signal with control, and e_{unctr} is the error signal without control.
The physical interpretation of this performance index is the attenuated power of the error signal after applying the control.

4. FXLMS APPROACH

The FxLMS algorithm has been originally proposed in (Morgan, 1980) and is described in detail in (Kuo and Morgan, 1996). The basic idea is to use a feedforward structure as shown in Figure 4.

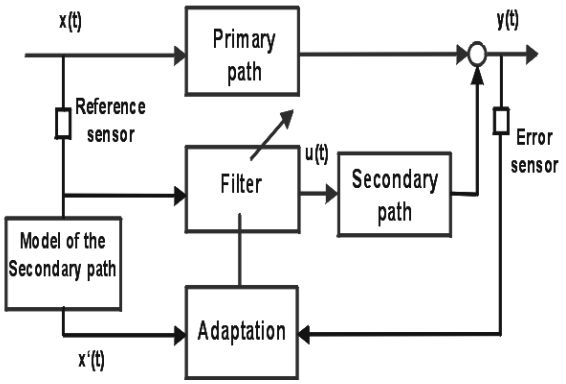

Fig. 4. Block diagram of FxLMS algorithm.

The transfer path between the disturbance source and the error sensor is called *primary path*. The *secondary path* is the transfer path between the output of the controller and the error sensor. The aim in the control loop is to minimise the output signal (error signal).

The adaptive filter has to approximate the dynamics of the primary path and the inverse dynamics of the secondary path. For the on-line adaptation of a FIR-filter (finite-impulse-response filter), two signals are used: error signal and reference signal filtered with the model of the secondary path (filtered-x).

The discrete-time transfer function of a FIR-filter has the form:

$$F(z) = \frac{U(z)}{X(z)} = \frac{w_0 z^m + w_1 z^{m-1} + ... + w_m}{z^m} \qquad (2)$$

whereas the vector

$$\mathbf{W}(k) = \left[w_0(k) \; w_1(k) \; ... \; w_m(k) \right]^T \qquad (3)$$

presents the filter coefficients vector.

The adaptation of the filter weights is performed through the well-known LMS (least mean square) algorithm originally proposed in (Widrow and Hof, 1960). The performance index J (internal for this approach) is built from the sum of squares of the sampled error signal:

$$J = \frac{1}{N} \sum_{i=1}^{N} y^2(i). \qquad (4)$$

This performance function, with respect to the vector $\mathbf{W}$ of filter coefficients, is described through a hyperparaboloid. An example is given in Figure 5. The optimal values for the adaptive filter coefficients are located at the deepest point of the performance surface. The LMS-algorithm searches on-line for the coordinates of the deepest point. The control signal is generated as the output of the adaptive filter.

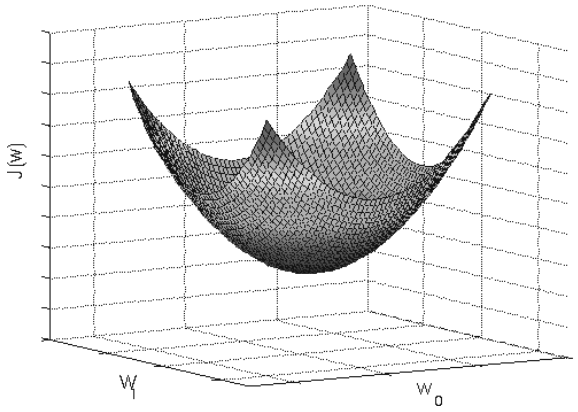

Fig. 5. Example of performance surface (here: for a two-weight system).

5. DISTURBANCE OBSERVER APPROACH

This method is based on state observer and state feedback. It is assumed that the disturbance enters at the input of the plant S (*secondary path*), see Figure 6.

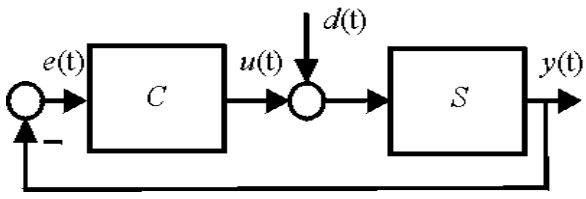

Fig. 6. Feedback loop.

The disturbance is modelled as a sum of a finite number of sinusoidal signals, which are harmonically related:

$$d(k) = \sum_{i=1}^{n} A_i \sin(2\pi f_i t + \phi_i), \qquad (5)$$

where n is the number of assumed harmonics, A_i and ϕ_i are the amplitude and the phase of the i-th harmonic and f_i the frequency of a single harmonic respectively.

This disturbance has a time-varying nature and requires that frequency measurement to be fed into the model. The frequency signal is taken from the engine control unit.

The disturbance attenuation is achieved through producing an estimate of the disturbance d and using this estimate, with a sign reversal, as a control signal u. To generate the estimate, a disturbance observer is used. The observer is designed off-line assuming time-invariance and investigating the property of robustness over a certain frequency region for a single observer. This is achieved by designing a stationary Kalman Filter (Kailath *et al.*, 2000). Later on, a gain-scheduling is implemented to cover the whole frequency region of interest by a stable observer. This provides a non-adaptive approach, where the frequency signal is used as a scheduling variable.

The transfer function of the controller C has infinite gain at the frequencies included in the disturbance model. The controller poles show up as zeros in the closed-loop transfer function. Figure 7 shows the frequency response magnitude of the sensitivity function $1/(1 + CS)$.

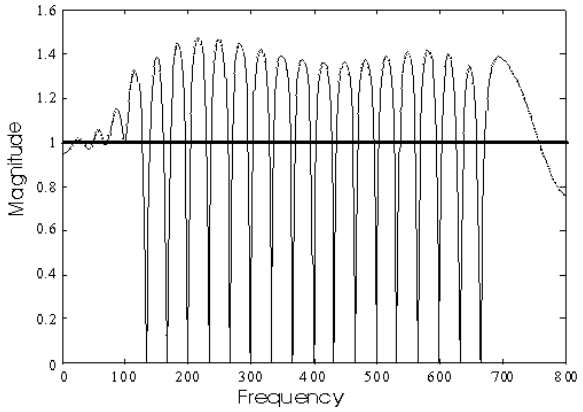

Fig. 7. Frequency response magnitude of the sensitivity function.

It is clearly seen that the magnitude of the sensitivity is zero for the frequencies specified in the disturbance model, which corresponds to complete disturbance cancellation. The improvement of the disturbance attenuation for these frequencies leads to some disturbance amplification between these frequencies. This effect is in accordance with Bode's well-known sensitivity integral theorem and is called waterbed effect (Hong and Bernstein, 1998). For more details on the algorithm, see (Bohn *et al.*, 2004).

5.1 Robustness to Measurement Errors in the Engine Speed Signal

The disturbance attenuation depends on the accuracy of the generated estimate. The engine speed signal driving the disturbance model plays an important role here. A robustness study on an artificial noise is presented here. This has been carried out as a simulation study with Matlab Simulink, since simulation conditions are repeatable. Later on, the result has been validated in a test vehicle by a real–time experiment. There was no noticable difference in the behaviour.

Figure 8 presents the analysis results of algorithm performance against percentage of an artificial white noise added to the original engine speed signal. The simulation has been done for a number of constant engine speeds.

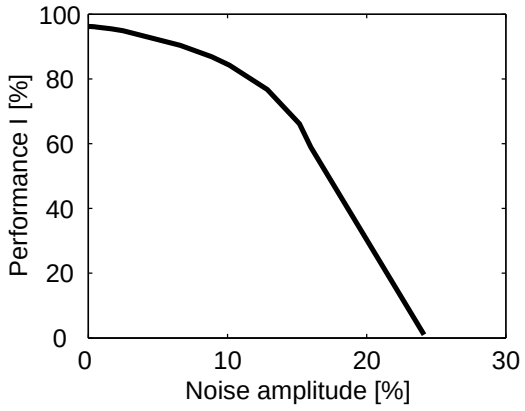

Fig. 8. Robustness to white noise applied to the engine speed signal.

The noise with a mean value equal to zero does not affect the accuracy of the estimation process significantly up to 10%.

One could also artificially change the signal by a constant offset. This condition has been simulated and the obtained results are presented in Figure 9. This simulation is done also for a number of constant engine speeds.

It is seen that the loss of performance is much larger here than in the white–noise case. This shows that the driving signal (fundamental frequency) needs to be very accurate, but up to 10% white noise is not critical.

6. ROBUSTNESS TO PHASE DELAY IN THE CONTROL SIGNAL

For both algorithms the effect of a phase delay in the control signal has been investigated. At the output of the controller a fractional–time–delay block has been implemented. A time–delay

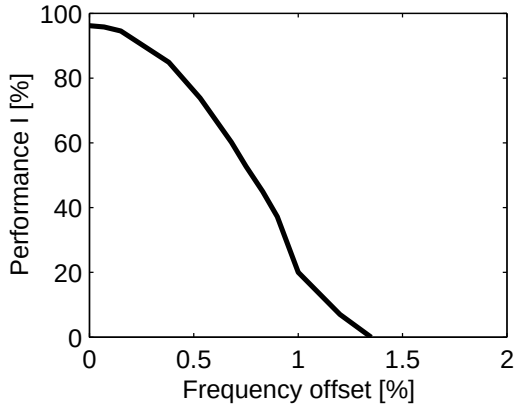

Fig. 9. Robustness to offset applied to the engine speed signal.

element has a transfer function with a unit magnitude and a phase delay depending on the frequency. For a constant engine speed, the time–delay block applies a linear phase delay with respect to frequency. Such a simulation has been done step by step increasing the time (phase) delay of the controller output signal. The obtained results are presented in Figure 10 for both algorithms.

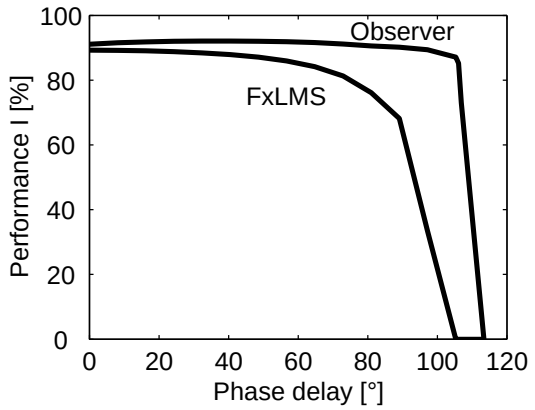

Fig. 10. Robustness to phase delay in the controller output.

On the basis of the obtained result one could notice that the disturbance–observer has not only a wider stability region, but also the smaller loss of performance against phase delay in the output signal of the controller. Both algorithms work well for a phase delay up to 40°. It has been also confirmed that the FxLMS algorithm stays stable for a phase delay up to 90°, which has been reported in the literature. See for example (Hansen and Snyder, 1997).

7. ROBUSTNESS TO UNCERTAINTY IN THE MAGNITUDE OF THE PLANT TRANSFER FUNCTION

The second criterion investigated for both algorithms is the robustness to uncertainty in the magnitude of the plant transfer function. The controllers were designed for the genuine transfer function $S(z)$ obtained through the identification experiment. In the simulation stage, the magnitude of the secondary path $|S(j\omega)|^*$ has been modified. A coefficient k is defined as the ratio of the varied magnitude to the genuine magnitude of the plant transfer function and given by the following equation:

$$k = \frac{|S(j\omega)|^*}{|S(j\omega)|}. \tag{6}$$

The dependency of the above defined performance index I on the magnitude ratio k is presented in Figure 11.

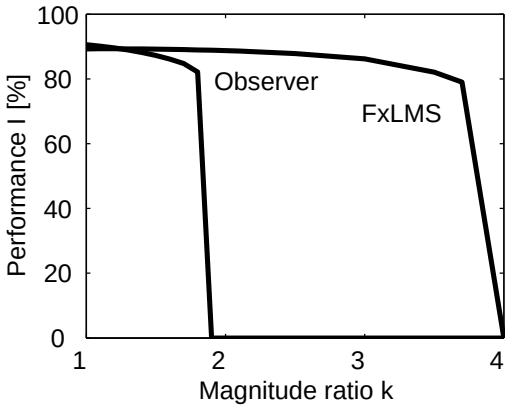

Fig. 11. Robustness to multiplicative variation in the magnitude of the plant transfer function.

The adaptation mechanism of the FxLMS algorithm makes this control technique more robust to magnitude umcertainty. A 3.5 fold increase in magnitude of the plant transfer function does not cause significant loss in the performance of the system. The disturbance–observer algorithm works well only for a ratio k lower than 1.8. This corresponds to the designed gain margin of 5 dB.

8. ROBUSTNESS TO VARIATION IN THE DAMPING RATIO OF THE RESONANCE IN THE PLANT TRANSFER FUNCTION

The plant, for which both controllers have been designed, has a resonance peak in a certain frequency region. The damping factor of the resonance in the secondary path used in the simulation has been modified. See Figure 12.

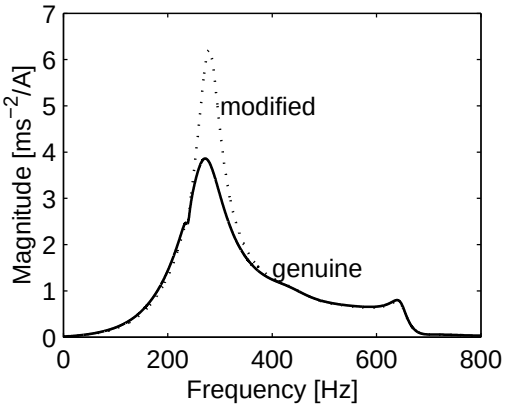

Fig. 12. Magnitude plot of the genuine and modified model of the secondary path.

A relative damping ratio d defined as a relation of the modified damping factor D^*_{res} at the resonance to the genuine one D_{res} has been chosen as a measure:

$$d = \frac{D^*_{res}}{D_{res}}. \tag{7}$$

On the basis of the obtained result presented in Figure 13 additional benefits of the FxLMS algorithm are apparent. Performance is maintained even if the damping ratio of the resonance decreases threefold.

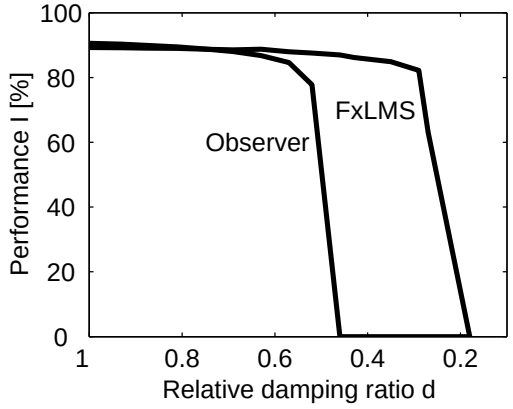

Fig. 13. Robustness to variation in the damping ratio of the resonance in the transfer function.

9. CONCLUSION

The paper has presented an experimental comparison of two different control techniques for active vibration control. Both work well in practice. Although the FxLMS has shown better robustness properties for a constant engine speed, the disturbance–observer technique results in a faster and a more accurate disturbance estimate and also disturbance attenuation, particularly for a time–varying fundamental frequency. This has been reported in (Bohn *et al.*, 2004). Due to a large number of influence parameters, no definite statements can be made with regard to which control scheme will be more suitable. Control strategy has to be chosen with regard to the characteristics of the vibration problem to be addressed, such as available sensor signals, type of excitation, frequency range of interest and spectral characteristics of excitations.

The purpose of this experimental analysis is the suitability of the components and the algorithms for the implementation of active vibration control systems in series production vehicles.

REFERENCES

Bohn, C., A. Cortabarria, V. Härtel and K. Kowalczyk (2004). Active control of engine-induced vibrations in automotive vehicles using disturbance observer gain scheduling. *Control Engineering Practice* **12**, 1029–1039.

Hansen, C.H. and S.D. Snyder (1997). *Active Control of Noise and Vibration*. E & FN Spon. London.

Hong, J. and D. S. Bernstein (1998). Bode integral constraints, collocation, and spillover in active noise and vibration control. *IEEE Transactions on Control Systems Technology* **6**, pp. 111–120.

Kailath, T., A.H. Sayed and B. Hassibi (2000). *Linear Estimation*. Prentice Hall. New Jersey.

Kuo, S.M. and D.R. Morgan (1996). *Active Noise Control Systems*. John Wiley and Sons. New York.

Lueg, P. (1936). Process of silencing sound oscillations. *U.S. Patent No. 2,043,416. Filed: March 8, 1934. Patented: June 6, 1936. Priority (Germany): January 1933.*

Morgan, D. R. (1980). An analisys of multiple correlation cancellation loops with a filter in the auxiliary path. *IEEE Trans. Acoust., Speech, Signal Processing* **28**, 17–27.

Sano, H., T. Tsuyoshi and M. Nakamura (2002). Recent application of active noise and vibration control to automobiles. In: *Proc. of the Active 2002*. Southampton. pp. 29–42.

Svaricek, F., C. Bohn, H.-J. Karkosch and V. Härtel (2001). Aktive Schwingungskompensation in Kfz aus regelungstechnischer Sicht. *at–Automatisierungstechnik* **49**, 249–259.

Widrow, B. and M. E. Hof (1960). Adaptive switching circuits. In: *IRE WESCON Conv. Rec.* pp. 96–104.